〈일반논문〉
Journal of the Korean Society of Visualization, Vol. 22, No. 1 (18~27), 2024
(Manuscript received : 2023.11.14./Revised : 2023.12.04./Accepted : 2023.12.04.)
DOI:http://dx.doi.org/10.5407/jksv.2024.22.1.018

ISSN 1598-8430 Print
ISSN 2093-808X Online

충격파 유동노출에 따른 황화납 나노소재의 미세구조 및 자기광학적 특성 분석에 관한 실험적 연구

김기원[*,‡] · 사크티벨[**,***,‡] · 사하데반[****] · 시바프라카시[*****] · 김익현[†]

Effect of Shock Wave Exposure on Structural, Optical and Magnetic Properties of Lead Sulfide Nanoparticles

Kiwon Kim[*,†], Surendhar Sakthivel[**,***,‡], J. Sahadevan[****], P. Sivaprakash[*****] and Ikhyun Kim[†]

Abstract A series of shock wave pulses with Mach number 2.2 of 100, 200, and 300 shocks were applied to lead sulfide (PbS) nanomaterials at intervals of 5 sec per shock pulse. To investigate the crystallographic, electronic, and magnetic phase stabilities, powder X-ray diffractometry (XRD), diffused reflectance spectroscopy (DRS), and vibrating-sample magnetometry (VSM) were employed. The material exhibited a rock salt structure (NaCl-type structure); XRD results indicated that material is monoclinic with space group C121 (5). Further, XRD results showed shifts due to lattice contraction and expansion when material was subjected to shock wave pulses, indicating stable material structure. Based on the data obtained, we believe that the PbS material is a good choice for high-pressure, high-temperature, and aerospace applications due to its superior shock resistance characteristics.

Key Words : Shock Wave(충격파), Stability Analysis(안정성 분석), Optical and Magnetic Properties (자기광학적 특성), Lead Sulfide(황화납), Nanomaterials(나노소재)

† Department of Mechanical Engineering, Keimyung University, Republic of Korea, Assistant Professor
E-mail: kimih@kmu.ac.kr
* Department of Mechanical Engineering, Keimyung University, Republic of Korea, Graduate Student
** Department of Mechanical Engineering, Keimyung University, Republic of Korea, Research Scholar
*** Centre for High-Pressure Research, Bharathidasan University, India, Research Scholar
**** Centre for Material Science, Karpagam Academy of Higher Education, India, Research Scholar
***** Department of Mechanical Engineering, Keimyung University, Republic of Korea, Postdoc Researcher
‡ K. K and S. S contributed equally to this work.

1. Introduction

In recent years, researchers have focused their attention on semiconducting nanoparticles for several compelling reasons including tunable size-dependent properties[1], highly efficient light emission[2], quantum confinement effects[3], sensing[4], etc. The field of semiconductor material technology research utilizes a diverse range of sulfide materials. Lead sulfide (PbS) semiconducting nanoparticles are inorganic nanoparticles that have garnered much attention in recent years[5]. Among

semiconducting substances, PbS is a special type of semiconductor, a binary IV-VI compound[6]. This material crystallizes in cubic structure with Fm3m No.225 space group and has a direct bandgap of 0.41 eV and Bohr radius of 18 nm. A significant blue shift of absorption onset is thus anticipated whenever the size of the crystallite is lower than the Bohr radius, the result of the size quantization effect[7]. Additionally, the wavelength at which the absorption edge occurs may be adjusted to from red to violet, spanning the full visible spectrum[8]. The transformation of PbS from a coarse-grained to a nanostructured form has significantly expanded the range of applications for the material, particularly in the field of infrared (IR) detectors and sensors[9], thermoelectric generators[10], photodetectors[11], optoelectronic devices[12], and solar cells[13].

Recent studies have shown that semiconducting sulfide nanoparticles are structurally stable at room temperature and pressure, but that their properties become highly unpredictable under non-ambient conditions[14]. It is crucial for both academic study and practical uses of crystalline materials to have a firm grasp of their polymorphic character, whether in bulk or nanoform. To determine the polymorphic qualities of a particular sample, static pressure and temperature driven phase transition techniques are commonly used[15]. Interestingly, there has been much research on PbS at ambient pressure and temperature, but investigations employing extreme conditions have been rare. Experiments carried out in dynamic shock conditions such as under extreme pressure and high temperature are important because they can shed light on material mechanical characteristics, phase changes, and responses to dynamic stress [16].

A shock wave is an energetic supersonic wave: when a large amount of energy is released quickly in a small area, it causes a shock wave, a high-energy supersonic wave that causes immediate shifts in the medium temperature, pressure, and density[17,18]. Shock waves differ from other common types of waves such as pressure waves and sound waves in how they behave and interact with materials[19]. Regardless of the distinctive nature of shock waves, the study of their effects when they come into contact with various materials has seen a significant surge in recent years, which has led to the development of a variety of new applications in such areas as biology[20], engineering[21], aerodynamics[22-24], and medicine[25].

The following is a summary of a few noteworthy findings, which will hopefully provide the reader with a better understanding of the significance of high-pressure research. Under shock wave exposed conditions, nanoparticles of corundum-type Fe_2O_3 (R-3c) go from having a weak ferromagnetic to a super paramagnetic nature. Researchers also discovered that there is a considerable reduction in particle crystallinity; this reduction is proportional to the number of shock pulses applied, which reached a maximum of 150[26].

There is currently no published investigative data on the effect dynamic pressure on PbS nanomaterials (NPs). This study outlines the process of measuring magnetic properties; it includes spectroscopic and diffraction investigations that can yield an understanding of the responses of magnetic materials subjected to shock wave pulses.

2. Experimental details

2.1 Material preparation and characterization

Nanomaterials of PbS with purity of 99.99 % were purchased commercially from Sigma Aldrich. A Rigaku XRD was used to measure X-ray diffraction for PBs NPS at 40 kV and 40 mA, with a CuKα monochromator set to 1.5406 wavelength. This device is a Powder X-ray diffractometer (PXRD), an effective tool that allows for the visualization of

structural changes in test specimens, particularly under dynamic shock-loaded conditions, and is used to investigate atomic-scale structural changes in crystalline and non-crystalline materials.

PbS commonly crystallizes in a rock salt structure (NaCl-type structure) at standard conditions (room temperature and atmospheric pressure); lead (Pb) and sulfur (S) ions are arranged in a cubic lattice. However, at high pressures and temperatures, material can undergo a phase transition to a new crystal structure. Furthermore, at various temperatures and pressures, PbS exhibits multiple crystal structures[27].

The chemical functional groups were investigated using Fourier-transform infrared spectroscopy (FTIR; Perkin-Elmer; Waltham, MA, USA). The specimens were imaged at ambient temperature in the range of 4000-400 cm^{-1}. Carl Zeiss sigma (2009) field emission scanning electron microscopy was used to analyze the PbS surface morphology.

FESEM combined with EDX spectroscopy was used to establish the elemental makeup of PbS nanomaterials. The FESEM technique was used to examine the surface morphological changes of the test sample because there is a high possibility of substantial morphological changes under shock wave-exposed conditions.

2.2 Shock tube tests

A shock tube is a simple device used to generate shock waves of a specified magnitude in a controlled laboratory setting[28]. There are three components to a shock tube: the driver, the driven part, and the diaphragm. When the driver part is filled with compressed gas until the diaphragm ruptures, a shock wave is generated and transmitted to the driven portion. As shown in Fig. 1, the NPs are positioned in the sample holder so that they are 2 cm from the end of the driven section. PbS NPs were subjected to shock waves,

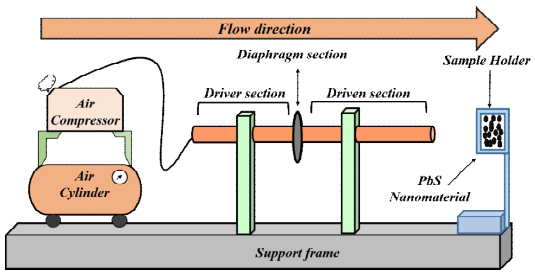

Fig. 1. Schematic of shock tube tests.

each with a Mach number of 2.2, over the course of 5 sec/pulses. We normally apply shock to materials based on the properties of the materials. Under shock wave flow conditions, materials typically exhibit great shock resistance or induce structural changes. The manually applied shock therefore occurred within a 5-second interval (i.e., 5 sec/pulses)[18,19,23]. The NPs were then subjected to several forms of investigation, including X-ray diffraction, FTIR, FESEM, PL, UV- DRS and magnetic measurements[29].

3. Results and discussion

3.1 Structural studies

Figure 2 presents XRD patterns of pristine (ambient) and shocked samples in the range of 20-60 angles at 40 kV and 40 mA, with a CuK♋ monochromator set to 1.5406 wavelength. XRD patterns show monoclinic structure with space group of C121 (5) in both the pristine and shocked samples. Additionally, each diffraction peak in the XRD pattern is indexed with the Miller Indices (hkl) values of the individual PbS of pristine and shocked samples and the detected crystalline peaks and their positions are confirmed to be aligned with the ICSD (68712) card number, confirming that the both control and shocked sample belong to monoclinic C121 space group.

The pristine XRD patterns make it abundantly evident that, under shocked conditions, neither lattice deformation nor crystallographic structural

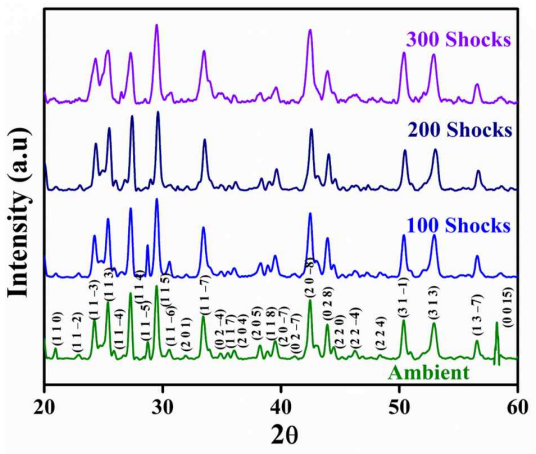

Fig. 2. PXRD patterns of pristine and shock wave exposed PbS NPs.

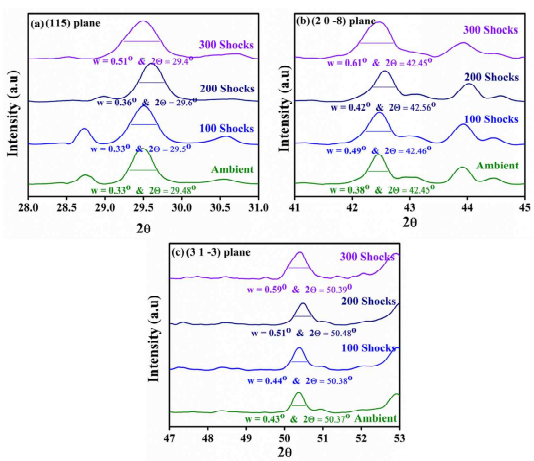

Fig. 3. Magnified PXRD patterns of pristine and shock wave loaded PbS NPs of different hkl planes (a) (1 1 5), (b) (2 0 -8) and (c) (3 1 –3).

transformation occurs. Furthermore, all crystalline peaks present in the control sample appeared because no new crystalline peak appeared, nor did any old peak disappear. The number of shock pulses induced a slightly higher angle shift, seen in the magnified image.

The corresponding zoomed-in XRD patterns are shown in Fig. 3 (a-c), in which shifts in the (1 1 5), (2 0 -8), and (3 1 -3) planes toward higher angles and peak broadening clearly demonstrate

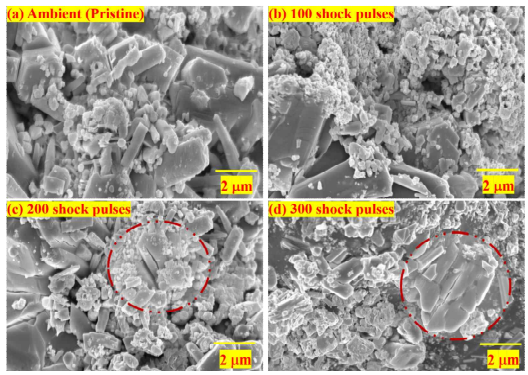

Fig. 4. FESEM images of (a) ambient (pristine) and (c-d) shock wave flow exposed samples.

the formation of a defective crystal structure under shocked conditions[30]. In general, lattice expansion, lattice disorder, and bond length expansion of the crystal structure occur when the diffraction peak shifts toward both higher and lower angle. Also, the crystal lattice can acquire dislocations and defects as a result of shock waves. Because they disturb the usual atomic arrangement, these atomic disruptions can cause localized atomic distortions and stress within the material[31].

Figure 4 presents FESEM images of the pristine and shocked samples. The morphology of the pure sample resembles a hollow, plate-like sphere. The surfaces of the pristine sample do not exhibit any obvious damage or deformation. Therefore, it is obvious that, before exposure to shock waves, the pristine and 100-shock samples were devoid of imperfections on the surface, of cracks, and of deformations.

At 200- and 300-shock pulse exposed conditions, large breakages were observed: cracks may have formed due to shock wave impacts. The pristine and 100-shock samples saw high dynamic impacts under shock wave loaded conditions; the unstable surface morphology led to several surface modifications such as deformations, cracks, shape changes, etc. The positions of major cracks are shown by red circles; corresponding SEM micrographs

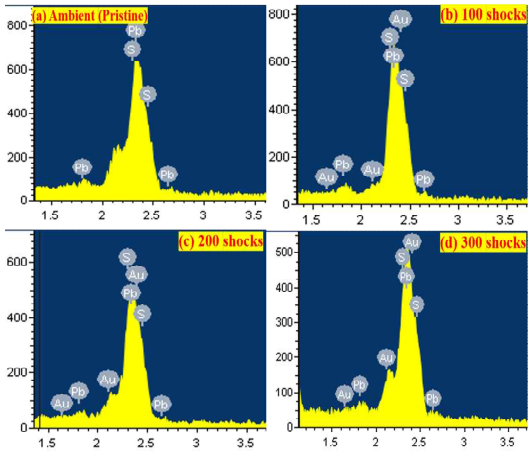

Fig. 5. EDAX spectra of (a) ambient (pristine) and (c-d) shock wave flow exposed samples.

are provided. However, certain cracks are extremely evident in the 2 μm range, and it was discovered that the crack level grew with increased number of shock pulses[19,32].

The particles in the sample experienced significant shock crushing due to strong transient pressure at a load of 300 shocks, and their forms completely changed. As shown in Fig. 4 (d), the rod-like morphological structures were considerably changes[33]. This was demonstrated by the large increase in particle fragmentation, which had a significant negative impact, causing surface defects and active areas on the surface. Further, for confirmation of the elemental analysis, the EDAX spectrum was obtained for pristine and shock loaded conditions, with results shown in Fig. 5 (a-d).

3.2 Optical properties

The photoelectrical characteristics of PbS NPs are studied using Ultraviolet Diffuse Reflectance Spectroscopy. Because the study of electronic devices requires extensive information on optical transmittance and optical band gap energy, we performed UV-DRS measurements between wavelengths of 200 and 900 nm. The resulting reflectance spectra

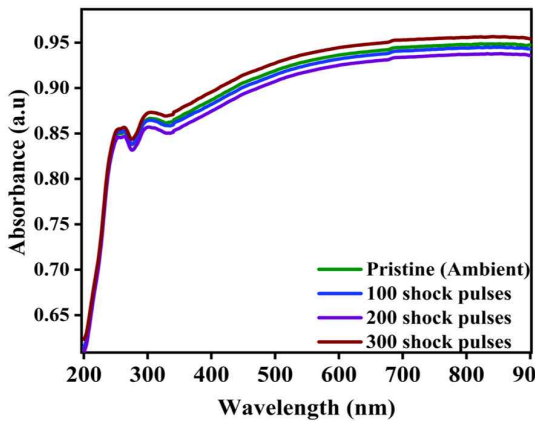

Fig. 6. UV-DRS spectra of ambient and shocked PbS NPs.

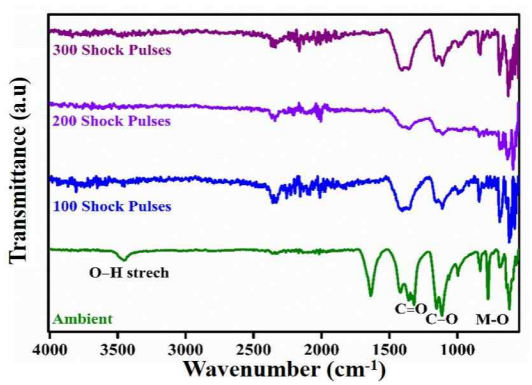

Fig. 7. FTIR spectra of ambient and shocked PbS NPs.

are shown in Fig. 6. The obtained ambient PbS NPs reflectance spectra matched well with those from earlier studies[34]. It is thus revealed that sample crystal structure and particle size are not impacted by the number of shock pulses; however, the proportion of reflectance changes slightly under shock wave loading conditions. The proportion decreases significantly at 100 and 200 shocks and then increases at 300 shocks.

The optical reflectance was measured in the range of 0 ~ 4000 cm−1, as shown in Fig. 7. After a shock wave, a remarkable decrease in the transmittance intensity was observed. This results from deterioration of the chemical structure and a

lowering of the molecular weight of PbS after the shock wave. We normalized the y-axis of all samples to check for chemical change of PbS after shock wave treatment; similar decreases in transmittance intensity are also found in the literature[35].

Characteristic peaks of PbS can be seen at 3451, 2326, 1640, and 1148 cm^{-1}, corresponding to O-H stretching, C-H stretching, C=O stretching, and C-O-C stretching, respectively. The bands at 1044 and 1046 cm^{-1} were caused by stretching vibrations of -O-C-C in PbS. The stretching of the -C-O-C- group in the ester linkages of PbS resulted in peaks in the region of 1144–1264 cm^{-1}. The band at the 1700 cm^{-1} region was attributed to C=O stretching vibrations of ester groups in PbS. Meanwhile, the peaks at 1359 cm^{-1} were assigned to symmetric and asymmetric deformational vibrations of –CH2– groups in the PBS main chains, respectively. Peaks in the 500–900 cm^{-1} region were identified as metal–oxygen (M–O) stretching vibrations.

A second sharp peak at 1395 cm^{-1}, absent in the shock samples, was identified as carboxyl group (C-O) stretching vibration. The peaks at 1044 to 1061 cm^{-1} and 1398 to 1431 cm^{-1} were due to the frequency of heteropolar diatomic molecules of PbS. And, the region from 1100 to 1128 cm^{-1} matched the C–N stretching vibrations. The region from 1560 to 1658 cm^{-1} corresponded to the water molecules[36]. The crystal lattice may vary under shock wave flow conditions, breaking up hydrogen bonds and changing the structure of the entire material. Vibrational modes associated with hydrogen bonding may thus be significantly altered or possibly removed, leading to the disappearance of corresponding FTIR peaks. Further, under shock flow conditions, as the crystal lattice undergoes compression or distortion, positions of atoms or molecules within the lattice can change. This can affect the vibrational frequencies of chemical bonds, leading to shifts in the FTIR peaks. These shifts are often associated with changes in bond lengths and bond angles within the material[37].

3.3 Photoluminescence analysis

Photoluminescence (PL) spectra of materials excited at 310 nm are shown in Fig. 8. The emission spectra show a distinct and broad peak; Gaussian curve fitting was used to deconvolute the PL spectra. The parent PbS deconvoluted into 4 components, PbS-100 and PbS-200 deconvoluted into 8 components, and PbS-300 into 7.

When exposed to shock waves, PbS first appeared to be displaced to the UV region; however, the highest shock wave sample actually had PL intensity in the blue indigo range. Green emission appeared to be absent from all shock waves samples. Considering the surface defects, the PL peak seen at approximately 424 nm was caused by transfer of electrons from the conduction band edge to holes trapped at interstitial Pb^{2+} sites. Further, the extreme pressures and temperatures generated by shock wave pulses must be the main sources of structural changes, phase transitions,

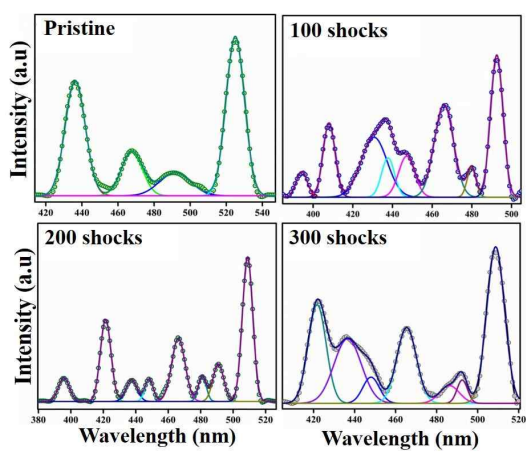

Fig. 8. PL spectra of ambient and shocked PbS NPs.

and disruptions in the material electronic properties, leading to the disappearance of peaks in the PL spectra of PbS samples under shock conditions. These changes may have an impact on the energy levels available for electronic transitions, which could cause some PL peaks to disappear. Peak disappearance in PL spectra can also be attributed to chemical processes, lattice distortions, and non-radiative relaxation processes under shock conditions.

3.4 Magnetic properties

Figure 9 shows measured room temperature hysteresis loops of the pristine and shock wave exposed samples. The magnetic characteristics of PbS NPs were evaluated using a vibrating sample magnetometer under shock wave loaded conditions. Magnetic measurements are performed in a Vibrating Sample Magnetometer (VSM) by placing a prepared sample on the VSM system. The magnetic response to an applied magnetic field can be measured using sample oscillation induced by the VSM. The observed hysteresis loop clearly shows that the ambient sample exhibits super paramagnetic behavior; the PbS NPs exhibits a large M-H curve loop at room temperature. It is interesting to observe that, when the number of shock pulses to the sample increased, such as to 100 and 200, the area of the hysteresis loop decreased, along with the saturation magnetization[38]. As a result, under shock wave flow conditions, an abundance of factors, including long-range order, local lattice vibrations, Jahn-Teller distortion effects, particle size, surface defects (spin canting), etc., significantly influence magnetic behavior and phase transformations[39].

The superparamagnetic behavior changed to diamagnetic behavior at higher shock conditions (300 shock pulses) due to unraveling of the alignment of magnetic moments within the

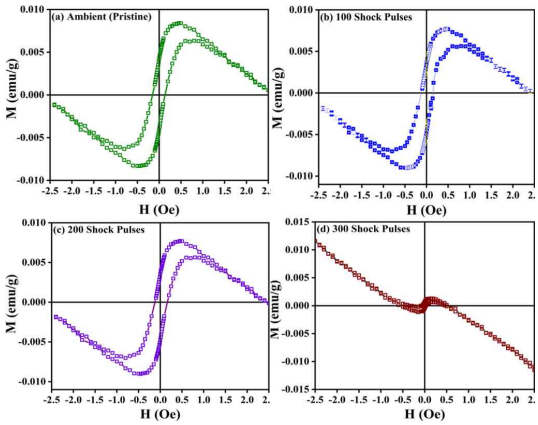

Fig. 9. Isothermal magnetization of PbS NPs. (a-c) Superparamagnetic behavior and (d) Diamagnetic behavior.

material under shock wave flow conditions. Due to lattice strain in the materials, we saw a shift toward a higher angle at up to 200 shock pulses, as show in results of XRD, FESEM, and UV-DRS measurements; these results are in good accord with the magnetic results. As shock to materials increased, we observed a relaxation of the material lattices[34]. The extremely high pressures and temperatures associated with shock events, during which PbS changed from super-paramagnetic to diamagnetic state, can also lead to changes in electronic structure, to spin interactions, and possibly to the introduction of defects or impurities within the material[23].

4. Conclusions

In this study, we have thoroughly investigated the structural, optical, morphological, and magnetic properties of commercially purchased PbS NPs at shock loads of up to 300 and a Mach number of 2.2. Powder XRD results confirm that the material has a monoclinic structure and is highly stable under shock loaded conditions. We observed shifts toward higher to lower angles due to lattice expansion and contraction. The same behaviors were observed in UV-DRS and PL measurements,

respectively. Further, particle size increased after 100 and 200 shock pulses and decreased after 300 shock pulses due to sudden changes in temperature and pressure under shock wave flow conditions. It was interesting to note that, under shock wave flow conditions, magnetic phase changed from super-paramagnetic to diamagnetic due to the alignment of magnetic moments within the material.

Acknowledgement

The research was supported by the National Res earch Foundation of Korea (NRF) grant funded by the Korea government (MIST) (No. 2022R1C1C10 06414).

REFERENCES

1) Yun, N., Kang, C., Yang, S., Hwang, S. -H., Park, J. -M. and Choi, T. -L., 2023, “Size-Tunable Semiconducting 2D Nanorectangles from Conjugated Polyenyne Homopolymer Synthesized via Cascade Metathesis and Metallotropy Polymerization,” J. Am. Chem. Soc., Vo.145(16), pp.9029~9038.
2) Ussembayev, Y. Y., Zawacka, N. K., Strubbe, F., Hens, Z. and Neyts, K., 2021, “Waveguiding of Photoluminescence in a Layer of Semiconductor Nanoparticles,” Nanomater., Vol.11(3), 683.
3) Sahadevan, J., Muthu, S. E., Kavu, K., Arumugam, S., Kim, I., Baby Sri Pratha, G. and Sivaprakash, P., 2022, “Structural, Morphology and Optical Properties of PbS (Lead Sulfide) Thin Film,” Mater. Today: Proc., Vol.64(5), pp.1849~1853.
4) Baraton, M. -I., 2006, “Metal Oxide Semiconductor Nanoparticles for Chemical Gas Sensors,” IEEJ Trans., Vol.126(10), pp.553~559.
5) Wattoo, M. H. S., Quddos, A., Wadood, A., Khan, M. B., Wattoo, F. H., Tirmizi, S. A. and Mahmood, K., 2012, “Synthesis, Characterization and Impregnation of Lead Sulphide Semiconductor Nanoparticles on Polymer Matrix,” J. Saudi Chem. Soc., Vol.16(3), pp.257~261.
6) Ezekoye, B. A., Emeakaroha, T. M., Ezekoye, V. A., Ighodalo, K. O. and Offor, P. O., 2015, “Optical and Structural Properties of Lead Sulphide (PbS) Thin Films Synthesized by Chemical Method,” Int. J. Phys. Sci., Vol.10(13), pp.385~390.
7) Sadovnikov, S. I., Gusev, A. I. and Rempel, A. A., 2016, “Nanostructured Lead Sulfide: Synthesis, Structure and Properties,” Russ. Chem. Rev., Vol.85, 731.
8) Chongad, L. S., Sharma, A., Banerjee, M. and Jain, A., 2016, “Synthesis of Lead Sulfide Nanoparticles by Chemical Precipitation Method,” J. Phys. Conf. Ser., Vol.755, 012032.
9) Göde, F., Yavuz, F. and Kariper, I. A., 2015, “Preparation and Characterization of Nanocrystalline PbS Thin Films Produced by Chemical Bath Deposition,” Acta Phys. Pol. A., Vol.128, pp.215~219.
10) Begum, A., Hussain, A. and Rahman, A., 2012, “Effect of Deposition Temperature on The Structural and Optical Properties of Chemically Prepared Nanocrystalline Lead Selenide Thin Films,” Beilstein J. Nanotechnol., Vol.3, pp.438~443.
11) Saran, R. and Curry, R. J., 2016, “Lead Sulphide Nanocrystal Photodetector Technologies,” Nat. Photonics, Vol.10, pp.81~92.
12) Jahromi, H. D. and Moaddeli, M., 2019, “Lead Sulfide; A New Candidate for Optoelectronics Applications in The Ultra Violet Spectral Range,” Mater. Res. Express, Vol.6(11), 116220.
13) Saikia, D. and Phukan, P., 2014, “Fabrication and Evaluation of CdS/PbS Thin Film Solar Cell by Chemical Bath Deposition Technique,” Thin Solid Films, Vol.562, pp.239~243.
14) Knorr, K., Ehm, L., Hytha, M., Winkler, B. and Depmeier, W., 2003, “The High-Pressure α/β Phase Transition in Lead Sulphide (PbS),”

Eur. Phys. J. B - Condens. Matter, Vol.31, pp.297~303.

15) Kim, H. J., Lee, J. B., Kim, Y. -M., Jung, M. -H., Jagličić, Z., Umek, P. and Dolinšek, J., 2007, “Synthesis, Structure and Magnetic Properties of δ-MnO2 Nanorods,” Nanoscale Res. Lett., Vol.2, pp.81~86.

16) Sivakumar, A., Sahaya Jude Dhas, S., Thirupathy, J., Sivaprakash, P., Anitha, K., Suresh Kumar, R., Arumugam, S. and Martin Britto Dhas, S. A., 2022, “Investigation on Crystallinity and Optical Properties of l-tartaric Acid Single Crystal at Dynamic Shocked Conditions,” J. Mater. Sci. Mater. Electron., Vol.33, pp.10841~10850.

17) Datey, A., Subburaj, J., Gopalan, J. and Chakravortty, D., 2017, “Mechanism of Transformation in Mycobacteria Using a Novel Shockwave Assisted Technique Driven by in-situ Generated Oxyhydrogen,” Sci. Rep., Vol.7, 8645.

18) Sivakumar, A., Eniya, P., Sahaya Jude Dhas, S., Dai, Lidong., Sivaprakash, P., Kumar, R. S., Almansour, A. I., Kalyana Sundar, J., Kim, I. and Martin Britto Dhas, S. A., 2023, “Comparative Analysis of Crystallographic Phase Stability of Single and Poly-Crystalline Lead Nitrate at Dynamic Shocked Conditions,” Mat. Sci. Eng. B, Vol.298, 116839.

19) Sivakumar, A., Sahaya Jude Dhas, S., Dai, L., Pushpanathan, V., Sivaprakash, P., Suresh Kumar, R., R., Almansour, A. I., Kim, I., Johnson, J. and Martin Britto Dhas, S. A., 2023, “Diffraction and Microscopic Studies on Lithium Sulfate Doped L-Threonine Under Dynamic Shock Wave Exposed Conditions,” Phys. B: Condens., Vol.665, 415065.

20) d’ Agostino, M. C., Craig, K., Tibalt, E. and Respizzi, S., 2015, “Shock Wave as Biological Therapeutic Tool: From Mechanical Stimulation to Recovery and Healing, Through Mechano Transduction,” Int. Surg. J., Vol.24, pp.147~153.

21) Ligrani, P. M., McNabb, E. S., Collopy, H., Anderson, M. and Marko, S. M., 2020, “Recent Investigations of Shock Wave Effects and Interactions,” Adv. Aerodyn., Vol.2, 4.

22) Kim, I., Park, G. and Na, J. J., 2019, “Experimental Study of Surface Roughness Effect on Oxygen Catalytic Recombination,” Int. J. Heat Mass Transf., Vol.138, pp.916~922.

23) Sivakumar, A., Sahaya Jude Dhas, S., Dai, L., P. Sivaprakash, P., Vasanthi, T., Vijayakumar, V. N., Suresh Kumar, R., Pushpanathan, V., Arumugam, S., Kim, I. and Martin Britto Dhas, S. A., 2023, “Structural Phase Stability Analysis on Shock Wave Recovered Single- and Polycrystalline Samples of $NiSO_4.6H_2O$,” JOM, Vol. 75, pp.4611~4618.

24) Devarajan, U., Sivaprakash, P., Garg, A. B., Kim, I. and Arumugam, S., 2023, “Investigation of Magnetic and Transport Properties of Co2FeSi Spin Glass Heusler Alloy Under Extreme Conditions,” J. Supercond. Nov. Magn., Vol.36, pp.1611~1618.

25) Kim, I. and Park, G., 2019, “Experimental Study of Oxygen Catalytic Recombination on a Smooth Surface in a Shock Tube,” Appl. Therm. Eng., Vol.156, pp.678~691.

26) Thiel, M., 2001, “Application of Shock Waves in Medicine,” Clin. Orthop. Relat. Res., Vol.387, pp.18~21.

27) Zheng, X., Gao, F., Ji, F., Wu, H., Zhang, J., Hu, X. and Xiang, Y., 2016, “Cu-doped PbS Thin Films with Low Resistivity Prepared via Chemical Bath Deposition,” Mater. Lett., Vol.167, pp.128~130.

28) Reddy, K. P. J., 2013, “Manually Operated Piston Driven Mini Shock Tube,” 28th International Symposium on Shock Waves, Vol.104, pp.561~565.

29) Sivakumar, A. and Martin Britto Dhas, S. A., 2019, “Shock-Wave-Induced Nucleation Leading

to Crystallization in Water," J. Appl. Cryst., Vol.52, pp.1016~1021.

30) Cho, S. H. and Kim, I., 2022, "Hypersonic Shockwave Robustness in Infrared Plasmonic Doped Metal Oxide Nanocrystal Cubes: Implications for High-Speed Ballistics Transport Applications," ACS Appl. Nano Mater., Vol. 5(12), pp.17487~17495.

31) Sivakumar, A., Sahaya Jude Dhas, S., Elberin Mary Thera, J., Jose, M., Sivaprakash, P., Arumugam, S. and Martin Britto Dhas, S.A., 2021, "Spectroscopic and Diffraction Studies of Polycrystalline Copper Sulfate Pentahydrate at Shocked Conditions," Solid State Sci., Vol.121, 106751.

32) Sivakumar, A., Sahaya Jude Dhas, S., Dai, L., Sivaprakash, P., Suresh Kumar, R., Almansour, A. I., Arumugam, S., Kim, I. and Martin Britto Dhas, S. A., 2023, "Sustainability of Crystallographic Phase of α-Glycine Under Dynamic Shocked Conditions," J. Mol. Struct., Vol.1292, 136139.

33) Sivakumar, A., Sahaya Jude Dhas, S., Lidong Dai, Sivaprakash, P., Suresh Kumar, R., Abdulrahman I. A., Arumugam, S., Kim, I. and Martin Britto Dhas, S.A., 2023, "Sustainability of Crystallographic Phase of α-Glycine Under Dynamic Shocked Conditions," J. Mol. Struct, Vol.1292, 136139.

34) Sivakumar, A., Sahaya Jude Dhas, S., Sivaprakash, P., Dhayal Raj, A., Suresh Kumar, R., Arumugam, S., Prabhu, S., Ramesh, R., Shubhadip, C. and Martin Britto Dhas, S. A., 2022, "Shock Wave Recovery Experiments on α-V2O5 Nano-Crystalline Materials: A Potential Material for Energy Storage Applications," J. Alloys Compd., Vol.929, 167180.

35) Giribabu, K., Ranganathan, S., Manigandan, R., Vijayalakshmi, L., Stephen, A. and Narayanan, V., 2012, "Hydrothermal Synthesis of Lead Sulphide Nanoparticles and Their Electrochemical Sensing Property," Adv. Mater. Res., Vol.584, pp.276~279.

36) Phua, Y. J., Chow, W. S. and Mohd Ishak, Z. A., 2011, "The Hydrolytic Effect of Moisture and Hygrothermal Aging on Poly (Butylene Succinate)/Organo-Montmorillonite Nanocomposites," Polym Degrad Stab., Vol.96(7), pp.1194~1203.

37) Bakshi, M. S., Thakur, P., Sachar, S., Kaur, G., Banipal, T. S., Possmayer, F. and Petersen, N. O., 2007, "Aqueous Phase Surfactant Selective Shape-Controlled Synthesis of Lead Sulfide Nanocrystals," J. Phys. Chem. C., Vol.111(49), pp.18087~18098.

38) Sivaprakash, P., Esakki Muthu, S., Saravanan, C., Rama Rao, N. V. and Kim, I., 2023, "The Effect of Mn on Structural, Magnetic and Magnetoresistance Properties of Ni–Mn–Sb Heusler Melt-Spun Ribbons Under Extreme Conditions" J. Phys. D: Appl. Phys., Vol.56(49), 495002.

39) Delhi Dona, E., Sivakumar, A., Sahaya Jude Dhas, S., Sivaprakash, P., Arumugam, S. and Martin Britto Dhas, S.A., 2021, "Sustainability of Corundum-Type Cr_2O_3 Nanoparticles at Shock Wave Loaded Conditions," Solid State Sci., Vol.119, 106701.